Trends in Applied Spectroscopy
Vol. 10, 2013

Original Communication

Fiber delivered excitation for laser induced incandescence measurements in ethylene premixed flame

Cosmin E. Dumitrescu[1] and Paulius V. Puzinauskas[2,*]

[1]Currently at Combustion Research Facility, Sandia National Laboratories, 7011 East Avenue, Livermore CA, 94550, [2]Mechanical Engineering Department, The University of Alabama, Tuscaloosa, AL 35487, USA

ABSTRACT

Laser-induced incandescence (LII) measurements using fiber-delivered laser pulses were made in an ethylene flame and compared under similar conditions to conventional open-optics measurements. For the same laser fluence, the signal magnitudes from the fiber delivered laser pulses were up to four times more intense and decayed faster than those from the open optics. However, when normalized with the intensity at maximum fluence, the fiber-delivered excitation LII (FDE-LII) signal showed similar relative laser fluence dependence with the conventional LII. The normalized signals from both methods also show very similar relative intensity variation profiles across the flame radius. These results indicate that the peak intensities of FDE-LII could be used in a very similar manner as conventional OO-LII to determine soot concentration; however additional analysis or development is required to infer the soot size characteristics from the signal decay rate.

KEYWORDS: laser induced incandescence, combustion diagnostics, fiber optics sensors, laser sensors, soot detection

INTRODUCTION

Laser-induced incandescence (LII) is an optical diagnostic technique used to determine soot particle size and concentration in combustion applications. Soot particles usually form aggregate structures where some bridging exists between the primary particles [1, 2]. When exposed to pulsed laser light, these aggregates absorb a portion of the incident energy and their temperature increases correspondingly, causing them to transfer energy to their surroundings via all three heat transfer modes. The associated incandescent radiation emission can be measured and analyzed to infer characteristics of the irradiated aggregate structures. This emission constitutes the LII signal. The peak LII signal intensity is proportional to particle concentration and its temporal decay is indicative of soot particle size so long as the particle temperatures are above those required for significant incandescent gray/blackbody radiation but less than those at which the particles begin to vaporize [3-6]. Using 1064 nm excitation, this condition is met with approximately 0.3 J/cm^2 laser fluence [7].

One of two methods is usually used to analyze the LII signal and characterize the emitting soot particles. The first method uses higher laser fluences to heat soot particles above the sublimation temperature (approximately 4000 K) and detects the LII signal at only one wavelength. A LII model simulating the soot particle heat transfer process is used to calculate the soot particle temperature. Then, with the temperature of the laser-heated region assumed uniform, the emission intensity at the calculated temperature is proportional to the soot concentration. This allows

*Corresponding author: ppuzinauskas@eng.ua.edu

quantifying relative concentrations spatially throughout a flame by repeating the measurement at different locations; however this method requires calibration with another technique (e.g. extinction measurements) to determine absolute soot concentration values [7].

The second strategy, called two-color emission pyrometry or two-color LII, uses low laser fluences to keep the maximum soot temperature below 3400 K at atmospheric pressure [8]. This technique, which is non-intrusive because it avoids soot sublimation, determines soot concentration through incandescence intensity measurements taken at two different wavelengths shortly after the laser pulse is fired. The soot temperature can be estimated from the ratio of the two intensity measurements based on Planck's law. Soot concentration is then obtained by comparing the absolute emission intensity at either of the two detection wavelengths with the theoretical emission intensity per unit volume of soot at the previously determined soot temperature. Temperature decay is used to determine soot morphology conditions.

The main advantages of the two-color emission pyrometry are that no other soot concentration method is required to calibrate the measurement and it gives more accurate information on soot morphology since higher laser fluence was demonstrated to significantly alter the soot structure [9].

To date, reported LII applications have used conventional exposed beam open optics to deliver the laser pulses necessary to generate LII signals to the measurement volume. These high energy nanosecond-pulsed laser beams must be carefully aligned and strict personal safety and equipment precautions must be implemented to avoid injury or equipment damage. The present work is motivated by the desire to ease these safety and alignment burdens associated with such exposed laser beams. A solution for remote optical diagnostics is to use flexible optic fiber for laser beam delivery. Maintaining the beam within a fiber optic guide will significantly improve the general safety of the implementation and reduce the required effort to obtain and maintain adequate beam alignment with the measurement volume. Ultimately, a probe could be constructed which contains both the beam delivery and the signal collection optics which could simply be moved to focus on different measurement volume targets. To our knowledge, LII studies using laser delivery via optical fiber have yet to be reported, most likely because standard solid optical fibers cannot deliver nanosecond pulses at the laser fluences required for LII. At high peak power, the nonlinearity in the refractive index of silica glass causes a self-focusing effect in the core region which results in irreparable damage to the fiber [10]. Recently, Matsuura *et al*. [11] have developed and manufactured a cyclic olefin polymer (COP) and silver coated hollow fiber with an indicated maximum transmitted energy for vacuumed-core conditions greater than 100 mJ with 9-12 ns FWHM pulses at a 10 Hz repetition rate. We have reported the first gas-phase laser-induced breakdown spectroscopy (LIBS) measurements using this fiber to deliver the spark [12, 13], and in this present study we use it to obtain fiber-delivered laser pulse LII measurements, which were made in a sooting ethylene flame.

LII signals resulting from laser pulses delivered both by fiber and open optics are compared under the same flame conditions. While the maximum laser fluence transmitted through the fiber was large enough to generate signals which could be processed using either of the LII analysis methods described above, these methods were not applied to determine the soot characteristics. Only the raw characteristics of the LII signals generated by the two laser delivery methods are presented and compared.

MATERIALS AND METHODS

The first harmonic of a Continuum Surelite I-30 Nd:YAG laser at 1064 nm (6 mm diameter, 30 Hz, 5-7 ns pulse width) was used to provide LII excitation in a premixed laminar ethylene flat flame. Figure 1 shows a schematic of the experimental setup. A half-wave plate in series with polarizing beam splitters reduced the laser energy to desired values. The laser-to-fiber coupling was achieved utilizing the same mechanism described in our LIBS investigation [13]. A brief description is included here for completeness. A retaining mechanism confines the fiber inlet into a sealed square tube which was

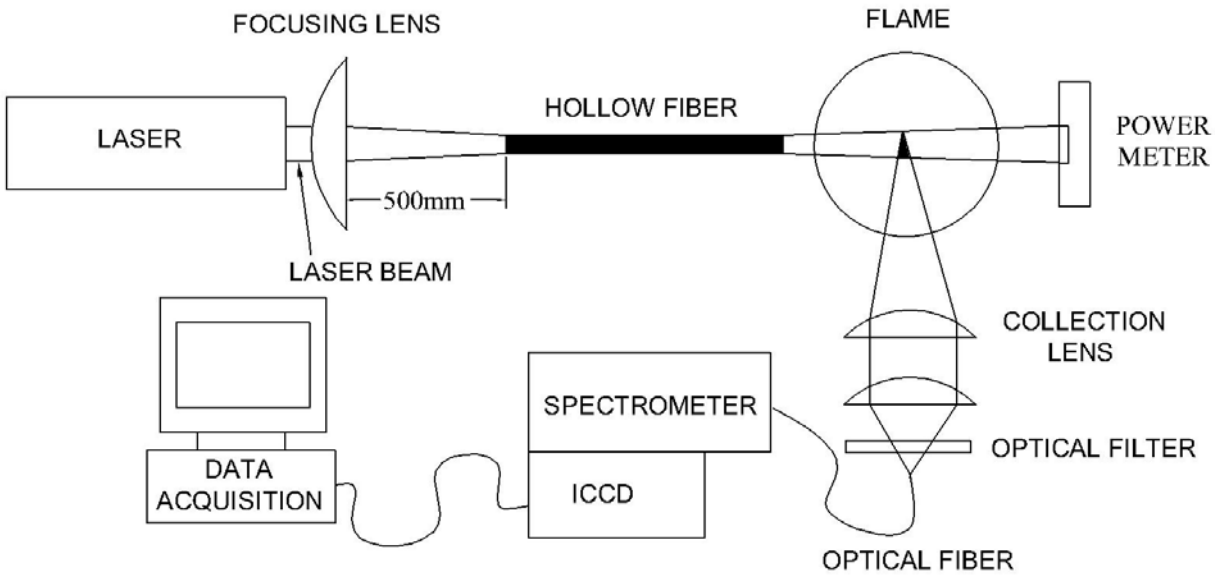

Figure 1. Experimental setup.

mounted onto a translational stage that allows 3-D movement for best fiber coupling. A small helium purge flows inside the tube and throughout the fiber to prevent laser breakdown at the entrance and inside the fiber. The other end of the fiber was clamped in front of the flame at the desired height and distance.

The fiber was kept straight for all the experiments reported here. The laser beam diameter was maintained constant inside the flame for both open-optics and fiber-delivered cases. The divergence of the beam exiting the fiber is $\theta \approx 7$ mrad ($M^2 \approx 12$). Placing the fiber end at 75 mm relative to the burner center resulted in a 3.5 mm diameter laser beam above the burner. For the open-optics LII (OO-LII) measurements, an f = 300 mm plano-convex lens inserted in the laser beam path created the same beam diameter and divergence above the burner as in the fiber-delivered excitation LII (FDE-LII) case. An Ophir 30(150)A-HE energy meter measured the laser beam energy delivered to the flame. Two plano-convex lenses (f = 100 mm, f = 50 mm, magnification $\times$ 0.5), placed orthogonally to the laser beam, collected emitted incandescence from a region corresponding to the center of the laser beam and focused it to a 1 mm diameter signal collection optical fiber bundle. A 488 nm narrow band filter (3 nm FWHM) placed before the optic fiber bundle avoided interference from the C_2 Swan bands emission at 473 nm (Δv = +1) and 516 nm (Δv = 0) [7]. The LII signal was then delivered to the entrance slit of a 0.3 m Acton SpectraPro-2300i spectrometer (0.5 mm slit) mated to a Roper-Scientific PI-MAX ICCD camera. The imaging system detected soot incandescence from a 2 mm diameter by 2 mm long cylinder within the laser beam's intersection with the flame. The ICCD camera was triggered by the laser and was setup to acquire individual (no ICCD accumulations) incandescence signals resulting from 1000 consecutive laser pulses. The data were taken with an ICCD gate width of 30 ns and a baseline gate delay of 30 ns after the start of laser pulse, both which were selected to maximize incandescence signal.

The laminar ethylene flame (Re ~ 260) was produced with a laboratory burner (25.4 mm diameter, 610 mm length). A short ceramic honeycomb section was inserted at the top of the burner tube to stabilize the premixed flame. A 102 mm long, 38.1 mm diameter chimney at the height of 65 mm above the burner increased the flame stability. The burner was mounted on a

horizontal 2D translator. The air and ethylene flow rates were 4.2 SLM and 0.67 SLM, resulting in a mixture equivalence ratio of Φ = 2.3. Both flows were controlled with Aalborg GFM47 digital flow meters. Spectrally resolved incandescence measurements from 485 nm to 491 nm were taken at 25 evenly spaced points across the flame diameter at 35 mm and 60 mm heights above the burner (HAB).

Considering the optical fiber energy-delivery limitations, the maximum laser fluence in this study was 0.4 J/cm^2 for both the OO-LII and FDE-LII.

RESULTS AND DISCUSSION

The determination of soot volume fraction through the LII analysis techniques described above is based on physical models which describe the heat and mass transfer processes in which a uniform laser beam profile is assumed. But consistent with what was presented in our LIBS work [12] the beam exiting the fiber in the present work appears to be a collection of hot spots, while the open-optics laser beam profile is nearly uniform, usually assumed to be a combination of Gaussian and 'top hat' shapes. This can be seen in Figure 2 which shows burn paper shots of fiber-delivered and open-optics laser beam at 0.2 J/cm^2 laser fluence.

If the beam characteristics were identical, it could be implicitly assumed that the open-optics and fiber-delivered laser pulses would yield identical LII performance. However, the evidence indicates beam quality differences associated with the two beam delivery methods, and thereby motivates this investigation to establish any effect these differences may have on LII performance.

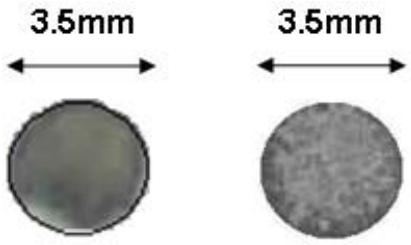

Figure 2. Laser beam burn paper shots at the measuring point: open-optics (left) and fiber-delivered (right).

As indicated in the introduction, LII signals are typically analyzed relative to their peak intensity and decay characteristics. Accordingly, the effect of laser fluence on peak intensity, the signal decay characteristics, and the LII profiles through a sooty flame were compared for the two beam-delivery methods in this investigation to establish any potential effect beam-delivery may have on LII analysis results.

Beam delivery method influence on laser fluence-peak LII signal relationship

To investigate the beam delivery's influence on the relationship between laser fluence effect and peak LII intensity, the peak signal intensity was measured as the laser fluence was increased from 0.05 to 0.4 J/cm^2 in 0.05 J/cm^2 increments, with the ICCD detection gate width and delay kept constant. Figure 3 shows that the incandescence signal for this particular location in the flame (~ 50% of the peak 40 mm HAB LII intensity) at the maximum laser fluence observed (0.4 J/cm^2) was two times larger for the FDE-LII compared with the conventional OO-LII, and nearly 3.3 times higher at the lower fluences (0.15 and 0.20 J/cm^2). This finding contradicts the open-optics results reported by Schulz *et al*. [7], who indicated a significant beam profile influence on the LII signal only above the vaporization threshold (0.4 J/cm^2 at 1064 nm).

If the LII signal is normalized from its peak at 0.4 J/cm^2, as presented in Figure 4, both laser beam delivery methods had a similar rate of LII signal increase with respect to fluence, with only the above noted points at 0.15 and 0.20 J/cm^2 substantially deviating from the curve. This finding suggests that the different beam profile has a large effect on the signal magnitude, but a much smaller effect on its relative variation with the laser fluence.

Beam delivery method influence on signal temporal decay

The LII signal temporal decay is used in soot measurement studies to derive the soot primary particle size, and it is dependent on soot particle size and fraction, its temperature and morphology, and the laser fluence [14]. To observe the signal temporal decay, the ICCD camera was triggered

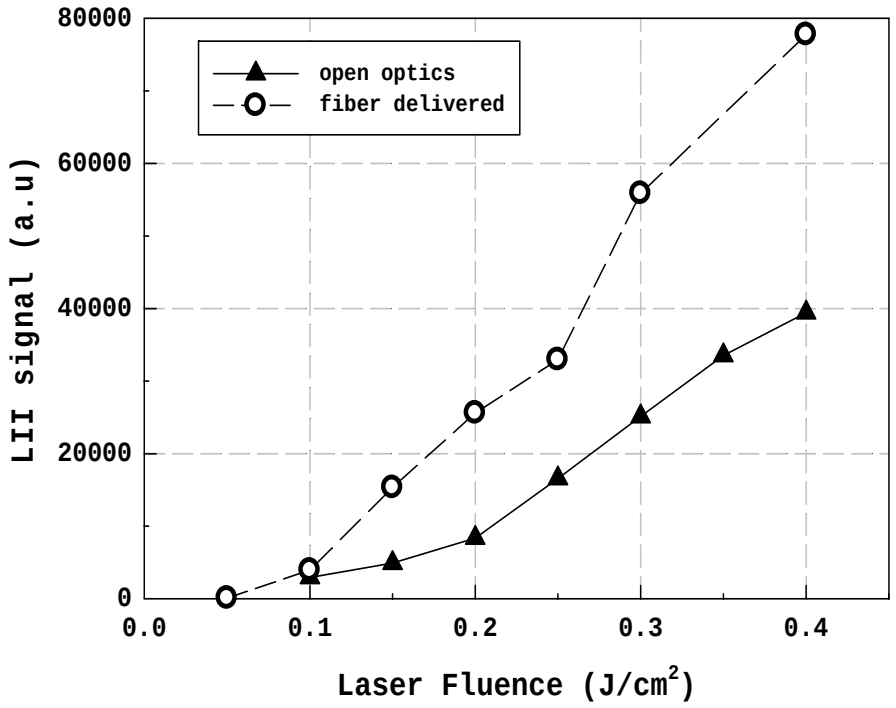

Figure 3. FDE-LII and OO-LII signal at different laser fluences (1064 nm, Φ = 2.3, HAB = 40 mm, R = 9 mm, gate delay and width 30 ns).

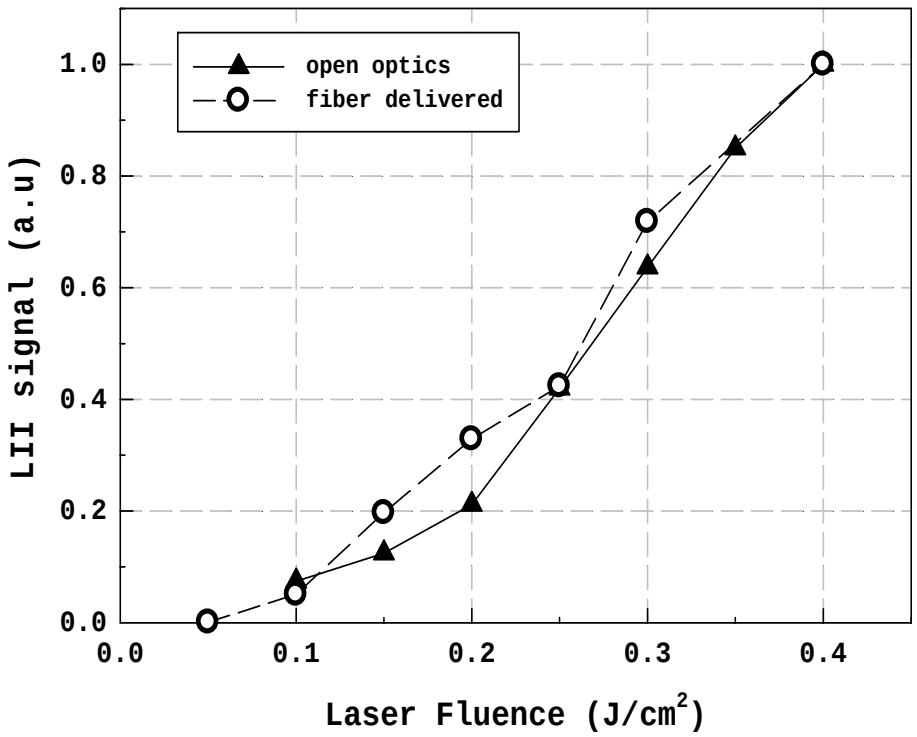

Figure 4. Normalized FDE-LII and OO- LII signal at different laser fluences (1064 nm, Φ = 2.3, HAB = 40 mm, R = 9 mm, gate delay and width 30 ns).

in a sequential mode. The detection gate was fixed at 2 ns, while the gate delay increased from the start of the laser pulse in 2 ns steps. Ten software accumulations were performed for each pair of detection gate and delay to increase the signal. The measurements were taken at a relatively low fluence (0.2 J/cm^2) and a radial position inside the flame (R = 5 mm, HAB = 60 mm) where good soot incandescence signal was expected.

Figure 5 shows that the FDE-LII signal decay rate was larger than the conventional OO-LII, which indicates faster soot particle cooling for the fiber-delivery LII heated soot. The FDE-LII signal being up to four times larger than the conventional LII, given the same fluence, suggests that the hot spots in the fiber-delivered beam locally heated the soot aggregates to a larger effective temperature than the OO-LII, possibly above the soot sublimation temperature. Regions of higher soot temperature for FDE-LII may result in partial sublimation and fragmentation of the particle structures, decreasing both the soot primary particle diameter and the average soot aggregate size inside the measurement area during and immediately after the laser pulse. This would affect the LII signal temporal decay similar to the simulations performed by Liu *et al.* [8], which showed that such a reduction in the soot primary particle diameter and soot aggregate size results in a faster temperature decay.

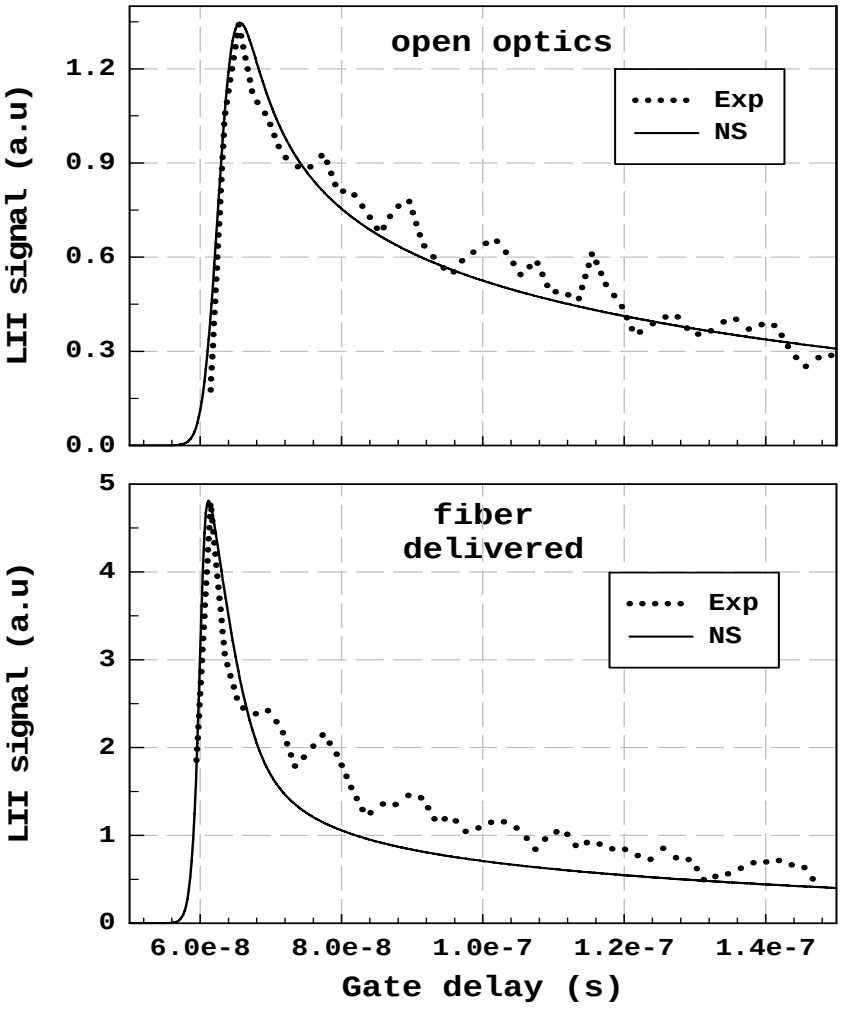

Figure 5. Experimental (Exp) and numerical simulation (NS) LII signal temporal decay for FDE-LII and OO-LII (1064 nm, Φ = 2.3, HAB = 60 mm, R = 5 mm, laser fluence 0.2 J/cm^2).

LIISim software was used to check this assumption by simulating LII signals temporal decay at similar conditions with the experiment. LIISim is a web-based LII-signal model developed by Schulz *et al*. [15] which solves the energy and mass balance equations for nano-sized particles heated by a pulsed laser and subsequently cooled by heat conduction, evaporation and radiation. Different options can be selected (mono and polydisperse particles, single particles or aggregates, heat conduction models) while setting physical input parameters, divided into absorption parameters (laser wavelength, beam diameter and fluence, soot absorption function), particle properties (density, initial temperature and diameter, number of primary particles per aggregate), gas-phase properties (temperature and pressure, thermal and mass accommodation coefficients) and detection bandpass. For the present study, the soot aggregate was modeled as a single particle with a monodisperse particle size distribution. The heat conduction was considered to take place in the free-molecular regime, with an initial particle temperature and soot primary particle diameter of 1700 K and 20 nm, respectively. The initial temperature and particle diameter were adjusted to optimize the agreement between the simulated and experimental results. The soot absorption function E(m) and thermal accommodation coefficient α were 0.35 [16] and 0.3, respectively, with a rectangular detection bandpass from 483 to 493 nm. Figure 5 indicates that for slightly lower laser fluence (0.15 J/cm^2 instead of 0.2 J/cm^2 as in the experiment) there is a good agreement between the experiment and the numerical simulation. If the simulated laser fluence was doubled (0.3 J/cm^2), there is a good agreement with the FDE-LII signal temporal decay. The maximum temperature indicated by LIISim was 3836 K and 4260 K, and the soot primary particle diameter was 20 nm and 18 nm for the OO-LII and FDE-LII, respectively. This is consistent with the hypothesis that even if the experiment was performed at relatively low laser fluence, the hot spots in the laser beam locally heated the soot aggregates above the soot sublimation temperature (~ 4000 K) and changed their size or morphology or both during and immediately after the laser pulse causing the change in cooling rate. This increase in the soot temperature also is likely responsible for the large increase in the measured LII signal. Overall, in this case the effect of the hot spots in the fiber-delivered beam profile was equivalent to a 100% increase in the laser fluence for a delivered laser fluence of 0.2 J/cm^2.

Beam delivery method influence on sooty flame LII profile

To determine if the beam profile influence on the LII measured signal is independent of the soot particle aggregate size, the LII signal was measured at two different heights above the burner (HAB) and different burner radial positions. The LII signal radial profile is presented in Figure 6. As was seen in Figures 3 and 5, the FDE-LII signal was substantially stronger than the OO-LII. In order to compare the relative change of the signal profiles for the two methods, they are plotted against different scales in Figure 6, with the FDE-LII on the left vertical axis and the OO-LII on the right. The scales were adjusted such that the maximum values for both methods fell at the same vertical position on the plot, meaning the plot effectively shows the profiles normalized relative to their maximum values, except with the signal strength values still available from the vertical axis scales. For both FDE-LII and OO-LII, the peak signal is detected at R ≈ 8 mm at HAB = 35 mm and at R ≈ 5 mm at HAB = 60 mm. The differences in signal intensities between the left and right side of the plot at HAB = 60 mm were caused by a slight tilting of the flame at the higher HAB to the left side in Figure 6 relative to the burner center-line found during the beam-to-burner alignment. Figure 6 also indicates a larger flame instability on the flame left side which widened the soot radial profile. Nevertheless, the evolution of soot radial profile with the height above the burner is in good agreement for both laser beam delivery methods and consistent with the soot evolution reported in other LII studies in laminar flames [4, 6-7], indicating that the relative response from the two delivery methods is similar for given soot concentration. At low heights (HAB = 35 mm) the soot particles are detected in the annular region of the burner corresponding to the fuel-rich side of the flame. The peak LII signal

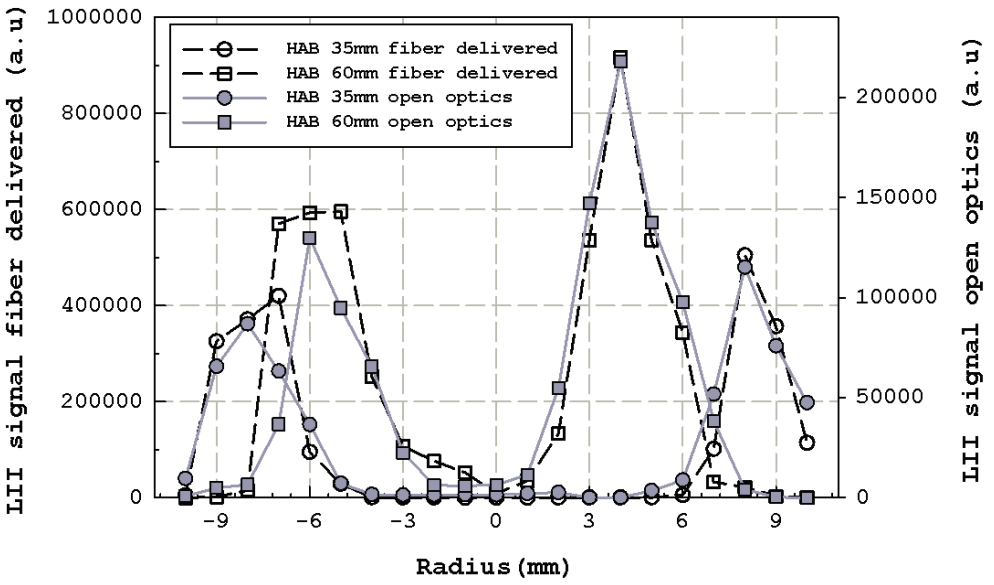

Figure 6. Measured incandescence signal for FDE-LII and OO-LII (1064 nm, Φ = 2.3, fluence 0.2 J/cm^2, gate width and delay 30 ns).

Table 1. LII peak signal intensity and standard deviation (Corresponding to R ≈ 8 mm at HAB = 35 mm and R ≈ 5 mm at HAB = 60 mm).

LII delivery method	HAB [mm]	$I_{peak,\ left}$ [a.u.]	$I_{peak,\ right}$ [a.u.]	I_{60}/I_{H35} Left	I_{60}/I_{35} Right	$\sigma_{relative}$	$\sigma_{relative}$
FDE-LII	35	371500	50500	1.60	1.82	0.52	0.18
	60	59600	916000			0.57	0.24
OO-LII	35	91000	120000	1.43	1.82	0.19	0.13
	60	130000	218000			0.32	0.21

moves closer to the centerline with increasing height (HAB = 60 mm) as the soot undergoes net growth [3].

As is evident from the vertical scales, the peak FDE-LII signal in Figure 6 is approximately four times larger than the OO-LII signal at both HABs. This was consistent with Figures 3 and 5, where the FDE-LII was 3.3 times larger at 0.2 J/cm^2 fluence in Figure 3 and 3.5 times larger at the peak values in Figure 5. The relative signal increase when the HAB increased from 35 mm to 60 mm was similar for both beam delivery methods (see Table 1), from 1.6 and 1.4 times on the left side of the flame for the FDE-LII and OO-LII, respectively, to 1.82 on the right side of the flame for both FDE-LII and OO-LII. The relative standard deviation (the ratio of standard deviation over the mean of the measurement) was almost the same on the more stable side of the flame (right side), and increased sharply for the left side flame FDE-LII measurements, confirming the flame instability during the experiment which resulted in the wider soot profile observed in Figure 6. The increased flame instabilities and standard deviation on the left side of the flame may also be responsible for the difference in signal magnitude between FDE-LII and OO-LII signal shown in Figures 3 and 5 because that was the flame region where the measurements for the laser fluence influence on LII signal were taken.

The above findings indicate that fiber-delivered beam profile hot spots do not adversely affect the measurement of relative soot concentration levels; however, they do affect the signal decay rates which will influence the ability to quantify particle structure. Since the exact morphology of the soot particles in the present flame is not known, it is not possible to address this issue further in this particular effort. Nevertheless, combined with the increase in the measured incandescence signal equivalent to a 100% increase in the laser fluence, reduced beam alignment and increased operational safety compared with conventional LII, the results demonstrated here indicate that with further development, FDE-LII could be an attractive choice for LII measurements.

CONCLUSIONS

LII measurements made using fiber-delivered laser pulses were compared to conventional open-optics measurements made under similar conditions. The signal magnitudes from the fiber-delivered laser pulses were two to four times greater, based on the position inside the flame, and decayed faster than those from the open-optics at the same fluence. The laser fluence dependence was similar for both laser pulse delivery techniques if the signals were normalized with their maximum values. The findings suggest that the hot spots in the fiber-delivered beam locally heated the soot aggregates to a larger effective temperature than the OO-LII, possibly above the soot sublimation temperature, even if the experiment was performed at relatively low laser fluence. This hypothesis was consistent with results obtained from LIISim, a web-based interface used to simulate LII signals temporal decay at similar conditions with the experiment. Calibration of the LIISim results to match the particular experiment simulated indicated maximum soot temperatures of 3836 K and 4260 K, and soot primary particle diameter of 20 nm and 18 nm for the OO-LII and FDE-LII, respectively. The large increase in the measured LII signal is believed to be caused by this increased effective soot temperature associated with FDE-LII. Overall, LIISim suggested that the effect of the hot spots in the fiber-delivered beam profile was equivalent to a 100% increase in the laser fluence for a delivered laser fluence of 0.2 J/cm^2.

The LII radial profiles at two different heights above the burner were similar for both laser pulse delivery techniques if the signals were normalized with their maximum values. This showed that the influence of the fiber-delivered beam profile hot spots on the LII measured incandescence did not affect the ability to quantify soot concentration, however the increased signal decay rate indicate the hot spots likely changed both the soot primary particle diameter and soot morphology.

These conclusions indicate that the fiber-delivery LII can be an attractive choice for LII soot concentration measurements compared with conventional LII due to (1) increased measured incandescence signal for similar laser fluences, (2) reduced beam alignment requirements and (3) substantially improved operational safety; however, further work is required to verify its ability to quantify particle size. This further work includes calibration with well-characterized particle aggregates and investigating performance with reduced fluence.

REFERENCES

1. Dobbins, R. A. and Megaridis, C. M. 1987, Langmuir, 3(2), 254-259.
2. Faeth, G. M. and Koylu, U. O. 1995, Combust. Sci. Technol., 108(4-6), 207-229.
3. Melton, L. A. 1984, Applied Optics, 23(13), 2201-2208.
4. Quay, B., Lee, T. W., Ni, T. and Santoro, R. J. 1994, Combust. Flame, 97, 384 -392.
5. Vander Wall, R. L. and Weiland, K. J. 1994, Appl. Phys. B, 59, 445-452.
6. Shaddix, C. R. and Smyth, K. C. 1996, Combust. Flame, 107, 418-452.
7. Schulz, C., Kock, B. F., Hofmann, M., Michelsen, H., Will, S., Bougie, B., Suntz, R. and Smallwood, G. 2006, Appl. Phys. B, 83, 333-354.
8. Liu, F., Yang, M., Hill, F. A., Snelling, D. R. and Smallwood, G. J. 2006, Appl. Physics B, 83(3), 383-395.
9. Michelsen, H. A., Tivanski, A. V., Giles, M. K., van Poppel, L. H., Dansson, M. A. and Buseck, P. R. 2007, Appl. Optics, 46(6), 959-977.

10. Matsuura, Y., Hanamoto, K., Sato, S. and Miyagi, M. 1998, Opt. Lett., 23, 1858-1860.
11. Sato, S., Ashida, H., Arai, T., Shi, Y.-W., Matsuura, Y. and Miyagi, M. 2000, Opt. Lett., 25, 49-51 .
12. Dumitrescu, C. E., Puzinauskas, P. V., Olcmen, S., Buckley, S. G., Joshi, S. and Yalin, A. P. 2007, Appl.Spectrosc., 61, 1338-1343.
13. Dumitrescu, C. E., Puzinauskas, P. V. and Olcmen, S. 2008, Appl. Optics, 47, G88-G98.
14. Snelling, D. R., Liu, F., Smallwood, G. J. and Gulder, O. L. 2004, Combust. Flame, 136, 180-190.
15. Hofmann, M., Kock, B. and Schulz, C. 2007, Proceedings of the European Combustion Meeting (Kreta, April 11-13, 2007), http://www.liisim.com
16. Crosland, B. M., Johnson, M. R. and Thomson, K. A. 2011, Appl. Physics B, 102(1), 173-183.